Electronic Supplementary Information

Determination of products

Detection of nitrate-N. [1] In order to adjust the absorbance to match the range of calibration curves, the electrolytes were diluted 12.5 times. Then, 0.1 mL 1 M HCl and 0.01 mL 0.8 wt.% NH_2SO_3H solution were added into 5 mL of diluted electrolyte. After 10 min, the absorption spectrum was recorded at wavelength of 220 nm and 275 nm. The final absorbance was confirmed by the following formula: $A = A_{220nm} - 2A_{275nm}$. The calibration curve of nitrate is measured by different concentrations of KNO_3.

Detection of nitrite-N. [1] First, 400 mg $C_6H_8N_2O_2S$, 20 mg $C_{12}H_{14}N_2 \cdot 2HCl$ and 1 mL H_3PO_4 was dissolved in the 5 mL water to form color developer. Then, 0.1 mL color developer was added into 5 mL of electrolytes which was diluted 20 times. When 20 min later, the absorbance was tested by UV-Vis spectrum and recorded at wavelength of 540 nm. The calibration curve of nitrate is measured by different concentrations of $NaNO_2$.

Detection of ammonium-N. [1] Nessler's reagent was used as color reagent for ammonium-N. A little of post-tested electrolyte was taken out and diluted 20 times. Then, 0.1 mL Nessler's reagent and 0.1 mL of 0.5 g/L $C_4H_4O_6KNa \cdot 4H_2O$ was added to 5 mL diluted electrolyte., and the mixture was left for 20 min. The wavelength of ammonium-N at 420 nm was confirmed using UV-Vis spectrum. And the calibration curve of nitrate is measured by different concentrations of NH_4Cl.

Isotope Labeling Experiments.

The isotope labeling nitrate reduction experiment was performed using $K^{15}NO_3$ as N-source to confirm source of N in ammonia. The electrolyte contained 0.5 M K_2SO_4 and 50 ppm $K^{15}NO_3$-^{15}N was added into electrolytic cell as the reactant. Then, the pH value of the cathode electrolyte was adjusted to 1~2 by 4 M H_2SO_4 after electrocatalytic procedure in order to confirm that the N-source is nitrate reduction. The standard reference material used is $K^{15}NO_3$and $^{15}NH_4Cl$.

***Calculation of yield, selectivity and Faradaic efficiency*:** The calculation source of all results is provided by the absorbancemeasured by the UV-Vis spectrophotometer.

The result of yield is obtained by Eq. 1:

$$Yiled_{NH_3} = (c_{NH_3} \times V)/(t \times m) \quad (1)$$

The result of conversion rate is obtained by Eq. 2:

$$Conversion_{NO_3^-} = \Delta c_{NO_3^-} / c_0 \times 100\% \quad (2)$$

The result of NO_2^- selectivity is obtained by Eq. 3:

$$Selectivity = c_{NO_2^-} / \Delta c_{NO_3^-} \times 100\% \quad (3)$$

The result of NH_3 selectivity is obtained by Eq. 4:

$$Selectivity = c_{NH_3} / \Delta c_{NO_3^-} \times 100\% \quad (4)$$

The Faradaic efficiency (FE) of nitrate reduction was obtained by Eq 5:

$$FE = (8F \times c_{NH_3} \times V)/(M_{NH_3} \times Q) \quad (5)$$

Here, $c_{NH_3}$is the mass concentration of NH_3 in the cathode electrolyte after the test, *V* is the volume of electrolyte in the cathode, M_{NH_3} is the molar mass of NH_3, t is the electrocatalytic time, m is the mass of the catalyst on the working electrode, $\Delta c_{NO_3^-}$ is the difference in the concentration of nitrate in the catholyte before and after electrocatalytic, c_0 is the actual concentration of nitrate in the conFig.d electrolyte, *c* is the concentration of nitrite or ammonia

in the catholyte after electrolysis, F is the Faradaic constant (96485 C mol^{-1}), Q is the total charge pass electrode during the electrochemical process.

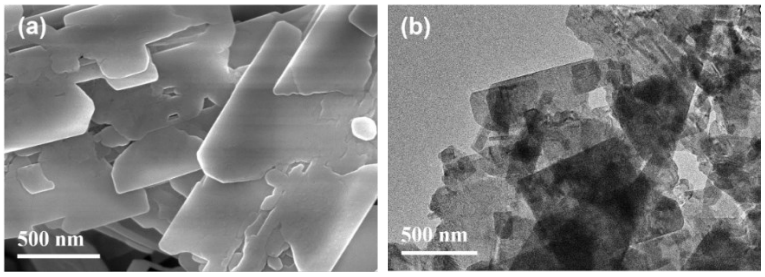

Fig. S1 (a) SEM image and (b) TEM image of CuO NPs.

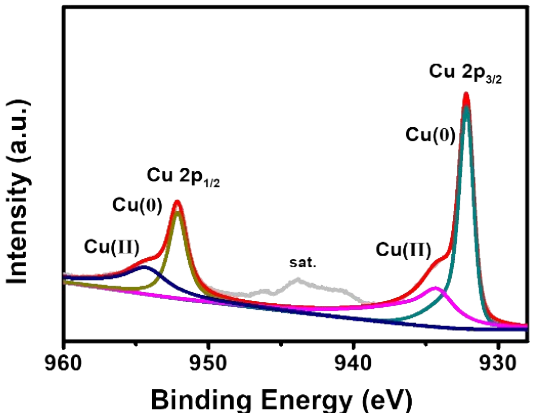

Fig. S2 Cu 2p XPS spectrum of *dr*-Cu NPs.

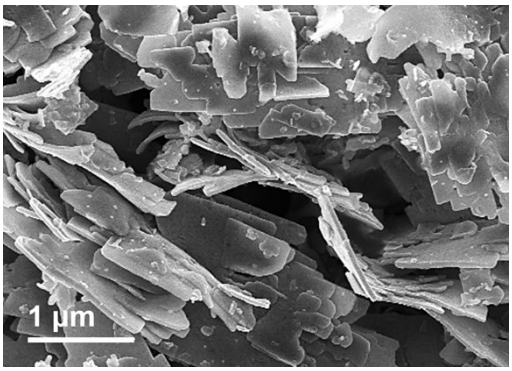

Fig. S3 SEM image of *dr*-Cu NPs.

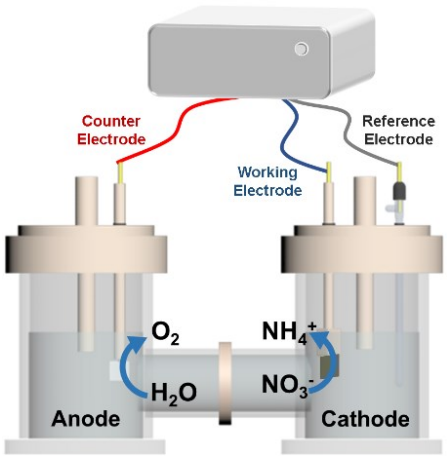

Fig. S4. The electrocatalytic reduction of nitrate to ammonia in an H-type electrolytic cell.

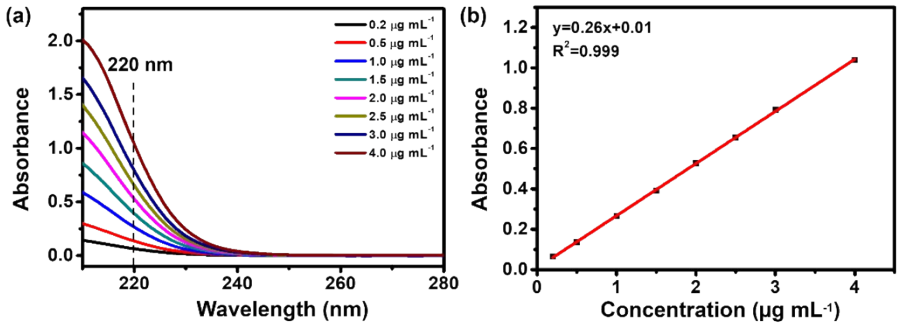

Fig. S5 (a) The absorbance of different $NaNO_3$ concentration ranging from 0.2 μg mL^{-1} to 4.0 μg mL^{-1} (b) The concentration-absorbance calibration curves of nitrate-N.

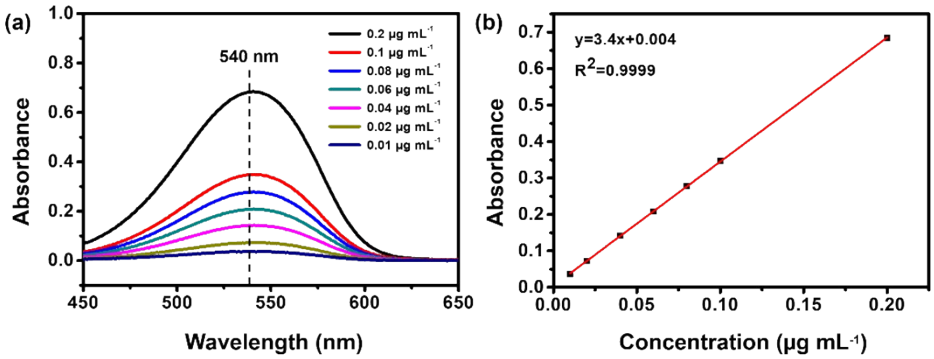

Fig. S6 (a) The absorbance of different $NaNO_2$ concentration ranging from 0.01 μg mL^{-1} to 0.2 μg mL^{-1} (b) The concentration-absorbance calibration curves of nitrite-N.

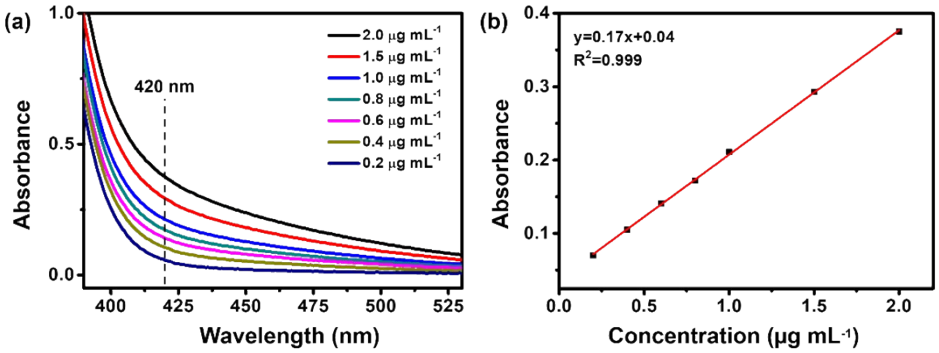

Fig. S7 (a) The absorbance of different NH_4Cl concentration ranging from 0.2 μg mL^{-1} to 2 μg mL^{-1} (b) The concentration-absorbance calibration curves of ammonium-N.

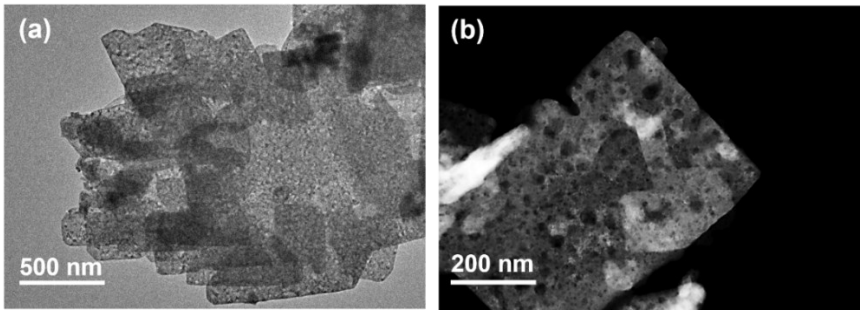

Fig. S8 (a)TEM image and (b) HAADF-SEM image of *dr*-Cu NPs after electrocatalytic nitrate reduction testing.

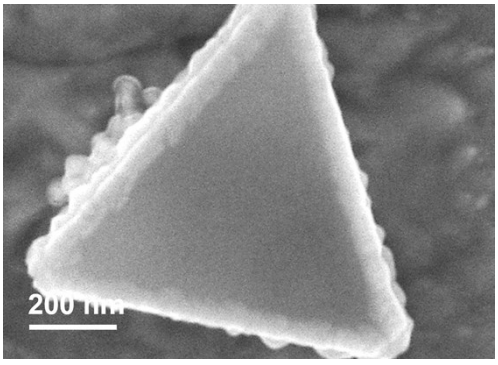

Fig. S9 SEM image of *df*-Cu NPs.

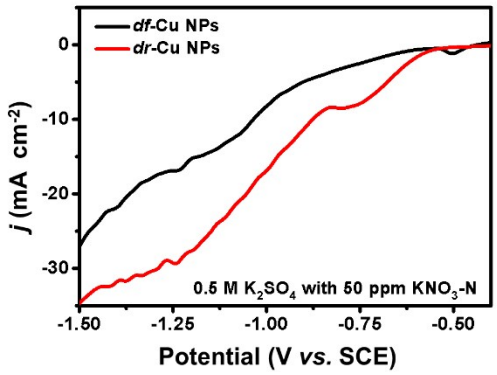

Fig. S10 LSV curves of *df*-Cu NPs and *dr*-Cu NPs in 0.5 M K_2SO_4 with 50 ppm KNO_3-N.

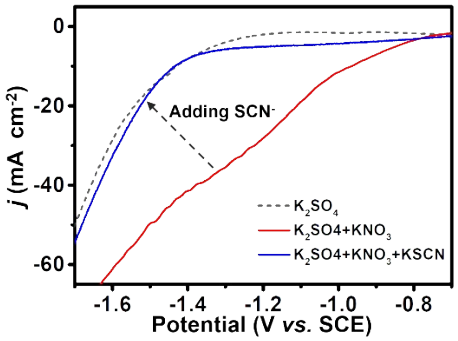

Fig. S11 LSV curves of *dr*-Cu NPs in 50 ppm KNO_3^--N with and without 50 ppm SCN^-.

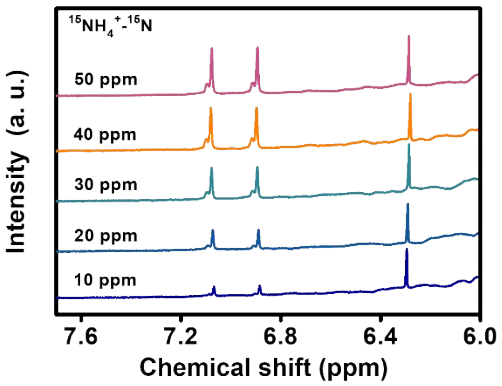

Fig. S12 The ^1H NMR spectra (600 MHz) of $^{15}NH_4^+$ with different $^{15}NH_4^+$-^{15}N concentration. he proton signal of maleic acid appears at δ = 6.31 ppm. The ^1H NMR spectra of $1^{15}NH_4^+$ showed double peaks at δ = 7.10 and 6.98 ppm.

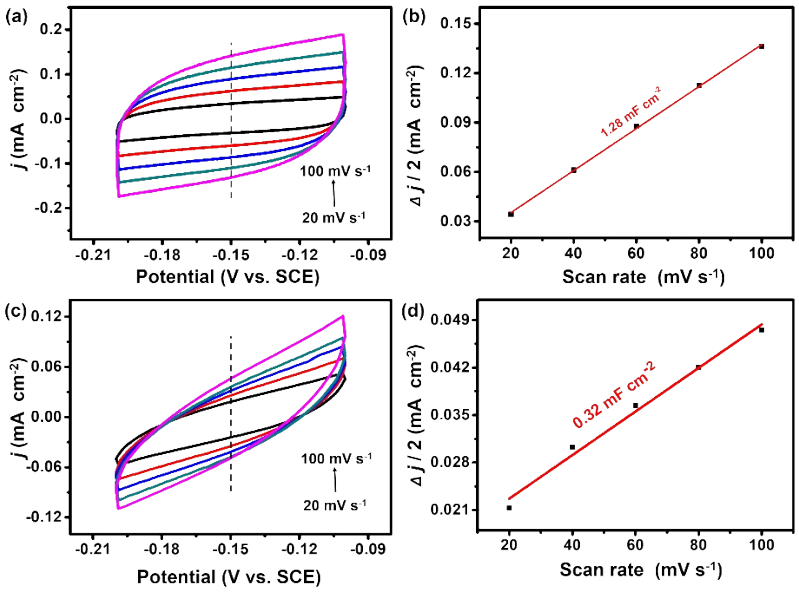

Fig. S13 (a) CV curves of *dr*-Cu NPs, (b) Plots of the current density versus the scan rate for *dr*-Cu NPs, (C) CV curves of *df*-Cu NPs with various scan rates from 20 to 100 mV s^{-1} and (d) Plots of the current density versus the scan rate for *df*-Cu NPs.

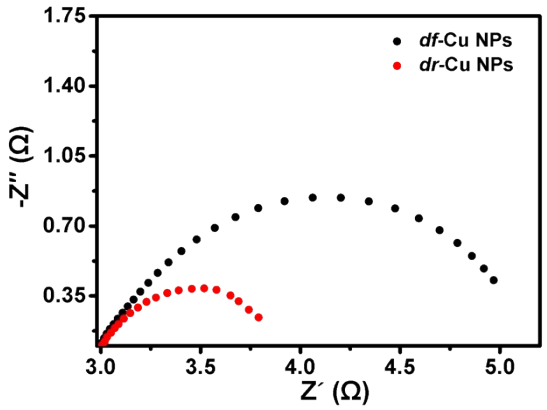

Fig. S14 EIS of *dr*-Cu NPs and *df*-Cu NPs.

Table S1 The comparisons of NO_3RR performance for the *dr*-Cu NPs and some other reported electrocatalysts.

Electrocatalyst	Electrolyte	NO_3^- conversion	Ammonia Selectivity	Ref.
***dr*-Cu NPs**	**50 ppm NO_3^--N + 0.5 M K_2SO_4**	**93.26%**	**81.99%**	**This work**
Fe	50 ppm NO_3^--N + 0.5 g/L Na_2SO_4	91%	28%	[2]
Pd-Fe foam	50 ppm NO_3^--N + 413 ppm K_2HCO_3 + 172 ppm $CaSO_4$	39.8%	92%	[3]
Fe (20%)@N-C	50 ppm NO_3^--N + 50 mM Na_2SO_4	83.0%	<75%	[4]
Cu/Ti + Cu/AC	50 ppm NO_3^--N	96.05%	62.64%	[5]
Cu/Ti	50 ppm NO_3^--N +0.5 mg/L Na_2SO_4	71.8%	N.A.	[6]
Ni-Fe^0@Fe_3O_4	50 ppm NO_3^--N + 10 mM NaCl	90.2%	10.4%	[7]
BDD	50 ppm NO_3^--N + 0.1 g/L Na_2SO_4	42%	8.9%	[8]
Pd–Cu/γAl_2O_3	50 ppm NO_3^--N	100%	19.6%	[9]
$Pd_{0.4}Cu_{0.6}$	50 ppm $NaNO_3$	N. A.	49%	[10]
Co_3O_4-TiO_2/Ti	50 ppm NO_3^- + 0.1 M Na_2SO_4 + PVP + 1000 ppm Cl^-	89%	24%	[11]
Cu/Ni/20-min	50 ppm NO_3^--N + 0.1 M K_2SO_4	97.2%	66.6%	[12]
Ni-TNTA	50 ppm NO_3^--N	89.6%	N.A.	[13]
Pt nanoparticle	50 ppm NO_3^--N	35%	N.A.	[14]

References

[1] Y. Wang, W. Zhou, R. Jia, Y. Yu, B. Zhang, *Angew. Chem. Int. Ed.* **2020**, *59*, 5350-5354

[2] W. Li, C. Xiao, Y. Zhao, Q. Zhao, R. Fan, J. Xue, *Catal. Lett.***2016**, *146*, 2585-2595.

[3] L. Rajic, D. Berroa, S. Gregor, S. Elbakri, M. MacNeil, A. N. Alshawabkeh, *Int. J. Electrochem. Sci.***2017**, *12*, 5998-6009.

[4] W. Duan, G. Li, Z. Lei, T. Zhu, Y. Xue, C. Wei, C. Feng, *Water. Res.* **2019**, *161*, 126-135.

[5] Q. Wang, H. Huang, L. Wang, Y. Chen, *Environ. Sci. Pollut. Res. Int.***2019**, *26*, 17567-17576.

[6] F. Liu, *Int. J. Electrochem. Sci.***2016**, 8308-8322.

[7] Z. A. Jonoush, A. Rezaee, A. Ghaffarinejad, *J. Clean. Prod.***2020**, *242*, 5998 – 6009.

[8] P. Kuang, K. Natsui, Y. Einaga, *Chemosphere* **2018**, *210*, 524-530.

[9] Z. Zhang, Y. Xu, W. Shi, W. Wang, R. Zhang, X. Bao, B. Zhang, L. Li, F. Cui, *Chem. Eng. J.***2016**, *290*, 201-208.

[10] J. F. Su, I. Ruzybayev, I. Shah, C. P. Huang, *Appl. Catal. B* **2016**, *180*, 199-209.

[11] J. Gao, B. Jiang, C. Ni, Y. Qi, Y. Zhang, N. Oturan, M. A. Oturan, *Appl. Catal. B* **2019**, *254*, 391-402.

[12] Y.-J. Shih, Z.-L. Wu, Y.-H. Huang, C.-P. Huang, *Chem. Eng. J.***2020**, *383*,123157.

[13] F. Liu, K. Liu, M. Li, S. Hu, J. Li, X. Lei, X. Liu, *Chemosphere* **2019**, *223*, 560-568.

[14] Q. Wang, X. Zhao, J. Zhang, X. Zhang, *J. Electroanal.l Chem.***2015**, *755*, 210-214.